ORIGINAL ARTICLE

Postnatal persistence of nonhuman primate sex-dependent renal structural and molecular changes programmed by intrauterine growth restriction

Andrew C. Bishop[1] | Kimberly D. Spradling-Reeves[1] | Robert E. Shade[2] |
Kenneth J. Lange[3] | Shifra Birnbaum[2] | Kristin Favela[3] | Edward J. Dick Jr[2] |
Mark J. Nijland[4] | Cun Li[5] | Peter W. Nathanielsz[2,5] | Laura A. Cox[1,2]

[1]Center for Precision Medicine, Department of Internal Medicine, Wake Forest School of Medicine, Winston-Salem, North Carolina, USA

[2]Southwest National Primate Research Center, Texas Biomedical Research Institute, San Antonio, Texas, USA

[3]Department of Pharmaceuticals and Bioengineering, Southwest Research Institute, San Antonio, Texas, USA

[4]Department of Obstetrics and Gynecology, University of Texas Health Science Center, San Antonio, Texas, USA

[5]Department of Animal Sciences, University of Wyoming, Laramie, Wyoming, USA

Correspondence
Laura A. Cox, Center for Precision Medicine, Department of Internal Medicine, Section on Molecular Medicine, Wake Forest School of Medicine, Winston-Salem, NC, USA.
Email: laurcox@wakehealth.edu

Abstract

Background: Poor nutrition during fetal development programs postnatal kidney function. Understanding postnatal consequences in nonhuman primates (NHP) is important for translation to our understanding the impact on human kidney function and disease risk. We hypothesized that intrauterine growth restriction (IUGR) in NHP persists postnatally, with potential molecular mechanisms revealed by Western-type diet challenge.

Methods: IUGR juvenile baboons were fed a 7-week Western diet, with kidney biopsies, blood, and urine collected before and after challenge. Transcriptomics and metabolomics were used to analyze biosamples.

Results: Pre-challenge IUGR kidney transcriptome and urine metabolome differed from controls. Post-challenge, sex and diet-specific responses in urine metabolite and renal signaling pathways were observed. Dysregulated mTOR signaling persisted postnatally in female pre-challenge. Post-challenge IUGR male response showed uncoordinated signaling suggesting proximal tubule injury.

Conclusion: Fetal undernutrition impacts juvenile offspring kidneys at the molecular level suggesting early-onset blood pressure dysregulation.

KEYWORDS
caloric mismatch, IUGR, kidney, nonhuman primate

1 | INTRODUCTION

Human epidemiological[1–3] and controlled maternal nutrient restriction (MNR) studies in rats, sheep, and nonhuman primates (NHP) show that sub-optimal intrauterine nutrition leads to intrauterine growth restriction (IUGR), altering fetal development and predisposing to later-life chronic disease, including renal and heart disease and hypertension[4–8] and chronic kidney disease.[9,10] In 2013, nearly 35 million Americans experienced either food insecurity or hunger,[11] including women of reproductive years. Developmental programming can be defined as *responses to challenges in critical developmental time windows that alter life course phenotype*. Poor maternal nutrition is a common programming challenge that leads to IUGR and adverse offspring life-course health.[12]

Studies of mechanisms by which MNR in the perinatal period negatively impacts offspring health have been mostly conducted in rodents[13] and are difficult to extrapolate to humans due to differences in rodent and primate renal developmental trajectories.[14] Renal molecular and cellular effects of combined prenatal and postnatal stressors remain uninvestigated in NHP, the species closest to human for the study of renal programming.

We have developed a well-characterized baboon model of moderate MNR (70% of chow fed to controls, CON) during pregnancy, resulting in IUGR and fetal renal,[15–18] cardiovascular,[19] metabolic,[20–22] hepatic,[23,24] and neural[25] phenotypes in female and male offspring.[18,25,26] By 0.5 gestation (G), the fetal kidney showed decreased tubule length and down-regulation of genes directing kidney branching morphogenesis[15] and mTOR nutrient sensing.[27] Renal programming effects persisted to 0.9 G.[17]

We hypothesized that fetal kidney molecular and tubular changes persist postnatally and are accompanied by dysfunction in renal development. We quantified kidney molecular pathways and function in IUGR and age-matched CON baboons (4.5 years; human equivalent 13 years). We evaluated responses when IUGR kidneys are subjected to the second-hit challenge of postnatal dietary mismatch with a high-fat, high-carbohydrate, high-salt (HFCS) Western-style diet and high fructose drink. We monitored food and drink consumption, body weight, and urine output. We also collected blood, urine, and kidney biopsies before and after the HFCS challenge to investigate molecular renal function with unbiased renal transcriptome and urine metabolome analyses. Our findings indicate that the impact of IUGR on female and male primate kidneys result in persistent renal dysfunction postnatally and response to HFCS differs by sex and fetal exposure.

2 | METHODS

2.1 | Ethics statement

The authors confirm that the ethical policies of the journal, as noted on the journal's author guidelines page, have been adhered to and all animal procedures were approved by the Institutional Animal Care and Use Committee at Texas Biomedical Research Institute and conducted in Association for Assessment and Accreditation of Laboratory Animal Care approved facilities at the Southwest National Primate Research Center.

2.2 | Animal selection and management

Details of baboon housing, individual feeding cages, training, and environmental enrichment were previously published.[28] Details on MNR development were previously published.[15] CON and MNR mothers spontaneously delivered CON and IUGR offspring, respectively, at full term. Offspring were reared with their mothers in group housing until weaning at approximately 9 months of age, and then maintained on chow diet in a juvenile cage with females and males until diet challenge.

2.3 | HFCS diet challenge

At ~4.5 years of age (human equivalent 13 years), 6 CON offspring (3 females, 3 males) and 6 age-matched IUGR offspring (3 females, 3 males) were challenged with a 7-week ad libitum HFCS diet, high fructose drink and water. The HFCS diet contained 73% Purina Monkey Chow 5038, 7% lard, 4% Crisco, 4% coconut oil, 10.5% flavored high fructose corn syrup, and 1.5% water. Vitamins and minerals were added to match the chow diet micronutrient composition. Palatability was enhanced using non-caloric artificial fruit flavors.[29] High fructose drink included water, high fructose corn syrup (2.83 Kcal/g, 76% sugar, 41.8% fructose, 34.2% dextrose, ISOSWEET 5500, Tate & Lyle), and artificial fruit flavoring.[29]

During the HFCS challenge, all baboons were run once per week into individual feeding cages, passing over an electronic weighing scale. Animals were fed ad libitum HFCS diet, high fructose drink, and water during the 13.5 h in individual cages. High fructose drink was provided in a Lixit waterer (Lixit) with a gauge to measure drink consumption for each animal. Food consumption was recorded for each animal.

2.4 | Cardiovascular telemetry

Due to budgetary constraints, telemetry was only measured in males. Based on other studies showing a greater impact of IUGR on male offspring,[30–32] we predicted that IUGR would impact male offspring to a greater degree than IUGR female offspring and chose to use telemetry for IUGR and CON males. Two weeks prior to initiation of the HFCS challenge, the male offspring received a radio transmitter (Model PA-C40, Data Sciences International, St. Paul, MN) capable of measuring arterial blood pressure, electrocardiogram (ECG), and temperature. A 2–3 inch midline incision was made on the abdomen below the navel and above the pubis to open the peritoneum. A 1–2 inch incision was made on the interior aspect of the right hind limb above the femoral artery. The sterile body of the transmitter was placed inside the abdominal cavity and anchored via attachment holes on the implant to the ventral peritoneal wall during closure of the peritoneal

incision. The pressure catheter exited adjacent to the peritoneal incision and was tunneled subcutaneously to the right hind limb incision. The femoral artery was dissected free and occluded at two points with suture material. A purse string of 3-O non-absorbable suture material was placed on the surface of the artery, and a small incision made in the center of the purse string. The catheter was introduced into the artery via the incision and the purse string used to seal the entry point. The catheter was then secured to surrounding connective tissue. ECG electrodes were also tunneled subcutaneously, one to the right shoulder and the other to the left groin. The skin incisions were closed in layers. Ketorolac was administered for pain management intramuscularly at the time of surgery (15-30 mg) and SID for 2 additional days, and Cephalexin (25 mg/kg) was administered twice daily for 7 days postoperatively via food.

Telemetry data were collected from the males weekly during the 13.5-h period the animals were in the individual feeding cages. Recordings were obtained 1 week prior to initiation of the HFCS diet and during each week of the 7-week challenge. Therefore, a total of 8 weekly measurements of ~13.5 h were made on each animal. One-minute recordings were averaged for 30-min time periods for each collection.

2.5 | Morphometric measurements

Morphometric measurements of each animal were collected before and after the HFCS challenge. Baboons were sedated with 10 mg/kg ketamine administered intramuscularly. To obtain the appropriate anthropometric measurements, hair was completely removed around the waist and hip circumference lines. Baboons were laid on a board with a flat surface, and body length (recumbent length) was measured using an anthropometer (cat. N101, Siber Hegner Ltd.) from the crown of the head to the right tibia. The head was positioned firmly against the fixed board of anthropometer in the extended position. The right knee was extended, and the feet were flexed at right angles to the lower legs. Length was recorded to the nearest 0.1 cm. Waist circumference was measured by applying a tape measure mid-way between the lowest point of the ribs in the mid-axillary line (costal margin) (10th rib) and the iliac crest in the mid-axillary line. Hip circumference measurements were taken at the point of maximum circumference over the buttocks with a non-stretchable tape held in a horizontal plane, touching the skin, but not indenting the soft tissue. Waist depth (anterior–posterior abdominal distance) was measured with the anthropometer from the plane of the back to the anterior point of the abdomen at the level of navel. Body mass index (BMI) was calculated by dividing the weight in kilograms by the crown-rump length in cm^2.

2.6 | Blood and kidney collections

Blood and kidney tissue samples were collected before and after the HFCS challenge at the same time as morphometric data were collected. Following an overnight fast, animals were premedicated with ketamine and then anesthetized with isoflurane (1.5% v/v, inhalation), and percutaneous venipuncture was performed on the femoral vein just caudal to the femoral triangle for blood sample collections. Percutaneous renal punch biopsies were also collected while the animals were anesthetized. The biopsy area was aseptically prepared, and the site of incision was locally infiltrated with lidocaine. The biopsies were then collected using ultrasound imaging to ensure consistent sampling among animals; kidney biopsies were frozen in liquid nitrogen and stored at -80°C until use. Specificity of kidney biopsy collections was determined based on gene expression specific for renal tubule segments.[33]

2.7 | Urine measures

Renal function was assessed using urine samples collected weekly while animals were housed in individual feeding cages. Urine volume measured, urine creatinine measured by Creatinine Colorimetric Assay Kit (Item # 500701; Cayman Chemical Co.), and urinary sodium and potassium concentrations were measured by flame photometry (Corning model 450) to calculate sodium and potassium excretion, respectively, for a 3-h urine collection period. Albumin concentrations were measured by Microalbumin Immunoturbidimetric Assay (Item #: KAI-057; Kamiya Biomedical Company) after instrument calibration (Item#: KAI-020C Microalbumin Calibrator; Kamiya Biomedical Company).

2.8 | Blood measures

Serum creatinine was quantified by Creatinine Assay Kit (Item # 700460, Cayman Chemical Co.), cortisol concentration by Immulite 1000 immunoassay kit (Item # 914038; Siemens Medical Solutions Diagnostics), and serum aldosterone excretion rates by radioimmunoassay (Diagnostic Products).[34]

2.9 | RNA isolation and microarray hybridization

Total RNA was isolated with quality checks, and complementary RNA (cRNA) was synthesized and biotinylated as described in[35] using HumanHT-12 v3 Expression BeadChips (Illumina, Inc.).

2.10 | Microarray data analysis

Gene expression data were extracted and log_2-transformed using GenomeStudio software (Illumina, Inc.) and analyzed using Partek® Genomics Suite (Partek®). Signal intensities were all-median normalized, and differentially expressed genes identified by analysis of variance (ANOVA; $p < .05$). Differentially expressed genes were overlaid onto canonical pathways and networks generated using

ingenuity pathway analysis (IPA; QIAGEN) Knowledge Base. Right-tailed Fisher's exact test was used to calculate enrichment of differentially expressed genes in pathways, $p < .01.$[36] Networks were built using the IPA Knowledge Base, requiring direct connections between molecules based on experimental evidence.

An end-of-pathway gene expression approach was used to identify coordinated pathways. We hypothesized that a pathway may only be relevant to the kidney phenotype if gene expression profiles after the pathway were consistent with the overall pathway change. Therefore, pathways meeting this criterion, as well as those downstream of these pathways, were investigated. If there were no differentially expressed genes after a pathway, that pathway was not considered relevant to the phenotype.[16]

Upstream regulatory network analysis was performed to identify potential causal networks which integrate previously observed cause–effect relationships, leveraging experimental knowledge about direction of effects to infer upstream regulatory molecules and potential mechanisms explaining observed gene expression changes. Z-scores predict regulatory directions and infer the activation state of a putative regulator. Detailed statistical models are provided.[37] Networks were considered significant for $p < .05.$

2.11 | Data sharing

The data supporting the finding of this study are openly available in repository Gene Expression Omnibus (GEO; http://www.ncbi.nlm.nih.gov/geo/)—GEO Series accession number GSE149895.

2.12 | Urine processing and metabolomics analysis

Urine metabolomics was performed on all samples except for a single baseline sample for one IUGR male due to technical issues. Urine samples were processed following previously published methodology.[38] Briefly, 10 ml urine aliquots were acidified to pH 2 with sulfuric acid. Metabolites were extracted with 2 ml of methylene chloride followed by a 30-s vortex. Samples were centrifuged, and the organic phase transferred to a new vial. 200 μl of the organic phase was transferred into sample vials containing sodium sulfate. For derivatization, 30 μl of dry pyridine and 200 μl of N,O-bis(Trimethylsilyl)-trifluoroacetamide (BSTFA) were added followed by incubation at 60°C for 60 min. Samples were injected onto a Pegasus 4D system equipped with an Agilent 7890 gas chromatograph (Agilent Technologies) in line with a LECO Time-of-Flight mass spectrometer (GC×GC-TOF-MS) (LECO Corp.).

2.13 | GC×GC-TOF MS system condition

The primary column was a 30 m × 0.25 mm i.d. × 0.25 μm d_f Rtx-1MS (Restek Corp.) and the secondary column a 2 m × 0.18 mm i.d. × 0.18 μm d_f Rxi-17M (Restek Corp.). Carrier gas was helium, and runs were performed in splitless mode. The initial temperature

of the GC oven was 40°C, held for 1 min, followed by ramping to 300°C at a rate of 5°C/min, followed by a 5-min hold. Secondary oven temperature offset was +5°C to the primary oven, and modulator temperature offset was set to +20°C of the secondary oven. The thermal modulation periods were set to 5 s, hot pulse time 0.6 s, and cool time between stages 1.9 s. Column flow was set to 1.0 ml/min, and the total run time was set to 34.80 min. The transfer line was set to 300°C and ion source 225°C. Acquisition rate was set to 100 spectra/s with a 500-s delay and mass range of 40–500 amu.

2.14 | Metabolomics data cleaning and analysis

MS data were generated and processed using Chromatof software v. 4.72 (LECO Corp), which included baseline correction, peak deconvolution, peak calling, and spectral library matching. Peak identification was assigned at a MS2 level consistent with spectra and fragmentation ions or accurate masses with proposed structure, as previously described.[39] Only spectral match scores equal or greater than 70% (forward score) to the NIST library were further considered. R-package, R2DGC,[40] was used to align identified peaks across groups.

Each alignment was exported to Excel for further processing. Alignments were filtered for metabolites present in at least 50% of samples and GC column and system contaminants were removed. The remaining compounds above background were normalized by the sum peak height of all annotated compounds. Putative compounds were assessed based on present/absent among sex and treatment groups. Normalized peak intensities present in all 3 samples of a group (e.g., all 3 males or all 3 females on HFCS diet,) were log transformed.

2.15 | Metabolomics pathway analysis

Identifiers from the Human Metabolome Database (HMDB)[41] and Kyoto Encyclopedia of Genes and Genomes (KEGG)[42] were inputted into MetaboloAnalyst 4.0[43] to determine common pathways present in the urine metabolomics analysis.

2.16 | Statistical analyses

Principal component analysis (PCA) and hierarchical clustering in Partek® Genomics Suite identified sex as the greatest source of variation in each dataset; therefore, we analyzed female and male data separately. Weight-adjusted fructose consumption was calculated by dividing the 7-week average fructose consumption by the 7-week average body weight. In addition, the percent change for weight and BMI, comparing the end of challenge to baseline, were calculated by dividing the end of challenge value by the baseline value, multiplying by 100 and subtracting 100. Pairwise comparisons were performed using two-tailed t-tests. Data from each diet group were analyzed independently for pre- and post-challenge means and evaluated using

two-tailed t-test and two-way ANOVA with significance $p < .05$ and marginal significance $.05 < p < .1$.

3 | RESULTS

3.1 | Kidney biopsy specificity

In previous rodent studies, transcriptome analysis of kidney microdissected renal tubule segments provided 626 renal nepron-specific genes[33]; our transcriptome analysis identified 447 of these genes were expressed in our baboon renal biopsy samples (Table S1).

3.2 | Sex differences for chow and HFCS

Kidney transcriptome analysis by PCA showed sex differences for both chow and HFCS where sex accounted for 53.0% of total variation for chow (Figure 1A) and 49.0% of total variation for HFCS (Figure 1B). Analysis of urine metabolome by PCA also revealed group clustering by sex, explaining 68.6% of total variation for chow (Figure 2A) and 71.1% of total variation for HFCS (Figure 2B).

3.3 | IUGR vs CON maintained on chow

3.3.1 | Morphometrics and renal function

At baseline, age-matched CON and IUGR female offspring were similar height, but IUGR weighed less and had lower BMI than CON (Table 1). Urine volume and urine creatinine were greater in IUGR than CON females (Table 2), while urine potassium (Table 2) and

serum creatinine (Table 3) were less. Urine albumin and creatinine/albumin ratios did not differ between IUGR and CON females (data not shown). Serum aldosterone and cortisol were similar between groups (Table 3). In males at baseline, age-matched CON and IUGR offspring were similar height and weight, but IUGR had lower BMI than CON (Table 1). Urine volume, urine potassium, serum creatinine, serum aldosterone, or serum cortisol were similar between IUGR and CON males (Tables 2 and 3); in addition, urine albumin and creatinine/albumin ratios did not differ between IUGR and CON males (data not shown). No differences were found for systolic, diastolic, and mean arterial blood pressure, and heart rate (Table 4).

3.3.2 | Renal transcriptome

In IUGR versus CON females, 687 genes were differentially expressed, 372 down and 315 up (Table S1). Four pathways were enriched for differentially expressed genes and passed the end-of-pathway criteria—3 down, including oxidative phosphorylation and mitochondrial function (Table S2).

Causal network analysis in IUGR versus CON females showed 2 networks: RB1 regulatory network was inhibited and the HOXA10 network activated in IUGR versus CON females (Table S3). Genes within this merged network were found in multiple signaling pathways including iron homeostasis, oxidative phosphorylation, glycolysis, and cell cycle control. The merged HOXA10 and RB1 inhibitory network shows the extent of overlap among genes (Figure 3).

In IUGR versus CON males, 1613 genes were differentially expressed with 600 down and 1013 up (Table S1). Five pathways passed end-of-pathway criteria—3 up-regulated pathways play roles in response to cell stress and DNA damage (Table S2). Figure 4 shows activation of BRCA1 in DNA damage signaling in IUGR versus CON males.
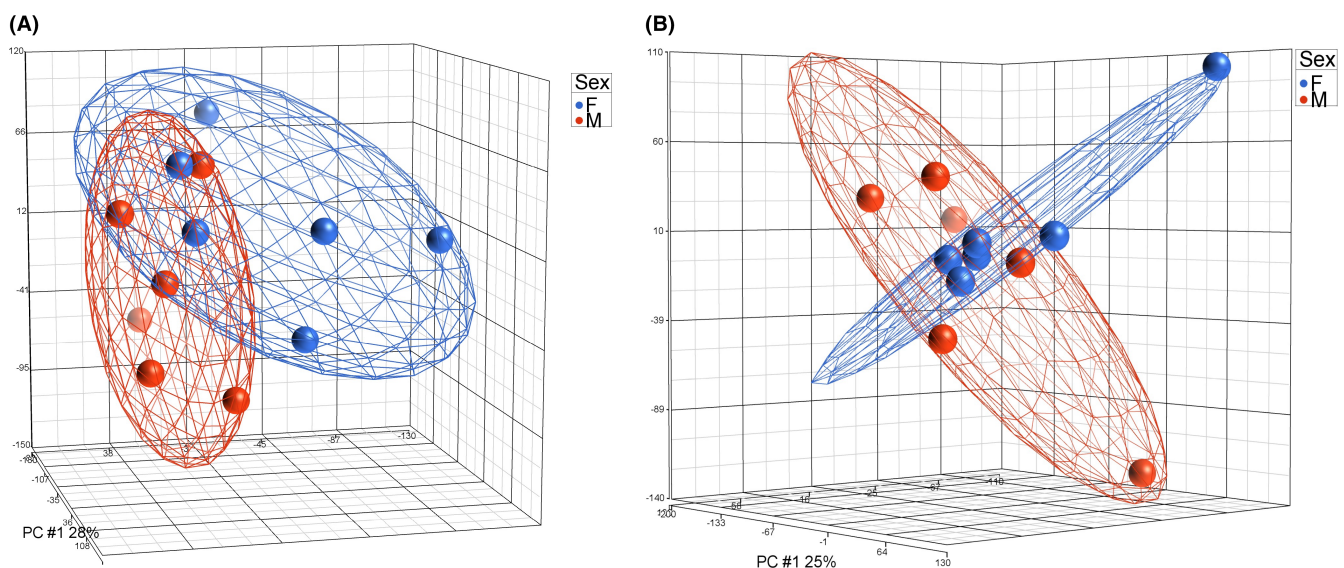

FIGURE 1 Principal component analysis (PCA) of sex differences within the renal transcriptome. PCA reveals sex differences in renal transcripts on both chow diet (A) and HFCS diet (B). Blue denotes females; red denotes males
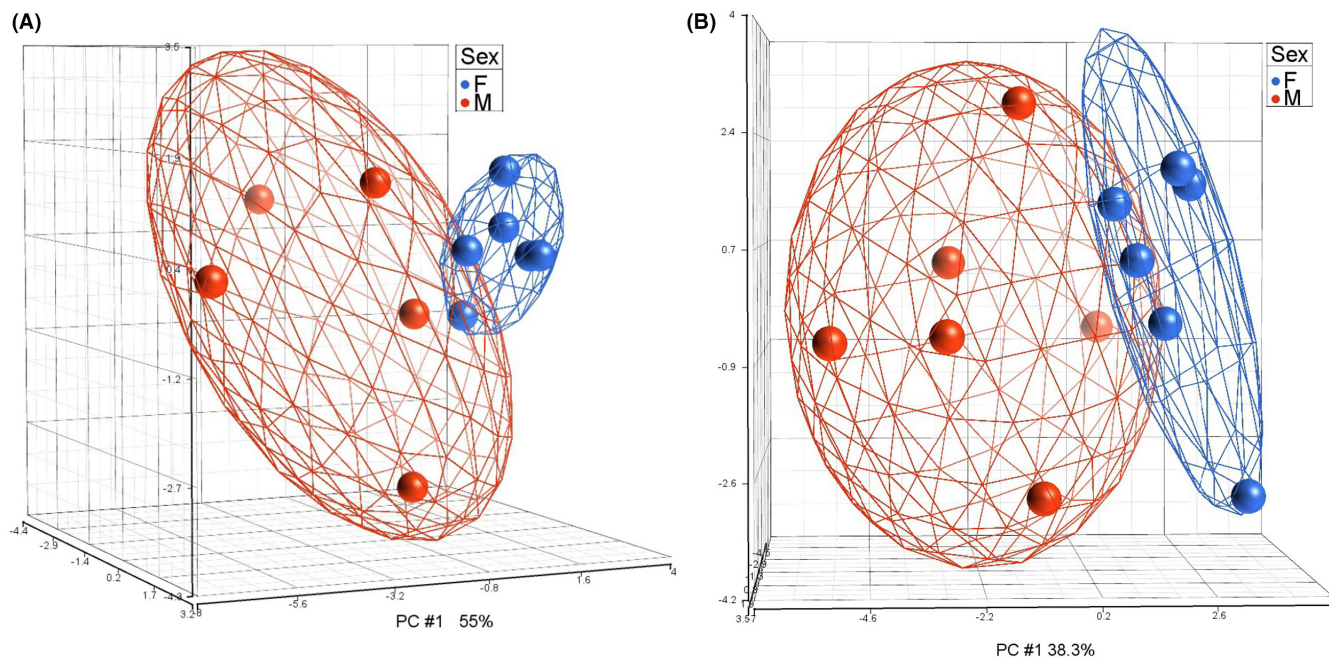
(A)

(B)

FIGURE 2 Principal component analysis (PCA) of sex differences within the urine metabolome. PCA reveals sex differences in urine metabolites signature on chow diet (A) and HFCS diet (B). Blue denotes females; red denotes males

TABLE 1 Morphometrics

		Height (cm)			Weight (Kg)			Body Mass Index		
		Mean	SEM	p-Value	Mean	SEM	p-Value	Mean	SEM	p-Value
F CON	Chow	87.8	3.35		12.9	0.61		16.70	0.49	
F IUGR		87.0	3.21	.87	9.9	0.95	.058	13.02	0.44	.005
M CON		90.1	0.46		15.0	0.85		18.45	1.16	
M IUGR		89.9	6.15	.98	12.0	1.86	.22	14.68	0.63	.046
F CON	HFCS	92.3	0.67		13.3	0.09		15.66	0.28	
F IUGR		90.8	2.13	.55	10.6	0.66	.015	12.86	0.19	.001
M CON		103.5	3.21		16.2	1.31		15.03	0.37	
M IUGR		96.7	4.26	.27	14.7	1.97	.56	15.53	0.82	.60
F CON	Diff	4.47	2.68		0.47	0.64		−1.05	0.21	
F IUGR		3.83	1.83	.85	0.73	0.38	.74	−0.16	0.26	.058
M CON		13.4	3.53		1.20	0.46		−3.42	0.89	
M IUGR		6.77	1.90	.17	2.67	0.12	.036	0.85	0.48	.013

3.3.3 | Urine metabolome in IUGR vs CON

Forty-seven metabolites were detected in females and males on chow diet (Tables S4 and S5). Of these, 6 were different and 2 marginally different; females were lower than males (Table 5). Sixteen metabolites were present in females on chow but not on HFCS diet. Ten metabolites were present in both sexes (Table 6, Table S5).

Thirty-six metabolites were detected in all female urine samples, while 15 were identified in all males (Table S5). In females, abundances of 2 metabolites (2-ethyl-p-xylene and decane) were higher in IUGR than CON, and 3 metabolites (hemimellitene, tridecane, and indane) were marginally different, with higher abundances in IUGR versus CON (Table 7).

3.4 | Response to the HFCS diet challenge

3.4.1 | Food consumption, morphometrics, and renal function

IUGR versus CON females were similar in food and fructose drink consumption during the HFCS challenge (not shown). Weight and BMI were less in IUGR than CON females after the challenge

TABLE 2 Urine measures of kidney function

		Urine Volume (ml/3 h)			Urine Creatinine Excretion (mg/kg/3 h)			Urine K Excretion (mmol/3 h/mg Cr)			Urine Na Excretion (mmol/3 h/mg Cr)		
		Mean	SEM	p-Value	Mean	SEM	p-Value	Mean	SEM	p-Value	Mean	SEM	p-Value
F CON	Chow	216.7	54.6		10.91	2.83		0.43	0.05		0.49	0.09	
F IUGR		411.7	69.4	.092	18.78	0.90	.057	0.24	0.002	.015	0.24	0.10	.15
M CON		370.0	90.7		15.43	2.38		0.38	0.07		0.46	0.15	
M IUGR		465.0	298.0	.77	14.99	6.90	.95	0.47	0.11	.53	0.62	0.23	.61
F CON	HFCS	258.3	22.0		12.91	2.80		0.33	0.07		0.42	0.17	
F IUGR		403.3	96.6	.22	18.32	3.26	.28	0.23	0.04	.28	0.62	0.33	.60
M CON		180.0	78.1		7.78	2.95		0.54	0.05		0.30	0.13	
M IUGR		216.7	112.0	.80	9.47	2.59	.69	0.38	0.02	.10	0.38	0.01	.65
F CON	Diff	41.7	50.2		2.00	3.72		-0.10	0.11		-0.08	0.08	
F IUGR		-8.3	39.2	.48	-0.46	2.38	.61	-0.01	0.04	.47	0.38	0.38	.31
M CON		-190.0	40.4		-7.65	2.37		0.16	0.10		-0.16	0.12	
M IUGR		-248.3	153.0	.57	-0.52	4.41	.23	-0.06	0.07	.14	-0.16	0.19	.99
F CON	7 wk avg	249.4	6.3		12.28	0.28		0.38	0.05		0.48	0.06	
F IUGR		300.2	18.7	.062	14.70	0.20	.002	0.24	0.03	.073	0.29	0.05	.072
M CON		283.3	22.4		12.20	0.15		0.32	0.03		0.44	0.03	
M IUGR		213.9	131.0	.63	8.78	3.16	.34	0.24	0.03	.13	0.53	0.05	.20

TABLE 3 Blood measures of kidney function

		Serum creatinine (mg/ml)			Aldosterone (% bound)			Aldosterone (pg/ml)			Cortisol (µg/dl)		
		Mean	SEM	p-Value	Mean	SEM	p-Value	Mean	SEM	p-Value	Mean	SEM	p-Value
Chow	F CON	1.19	0.08		0.20	0.03		194.23	39.28		37.17	3.92	
	F IUGR	0.88	0.11	.084	0.30	0.10	.40	176.87	126.58	.90	33.60	1.35	.44
	M CON	0.94	0.06		0.48	0.04		33.06	8.19		43.03	3.67	
	M IUGR	1.09	0.16	.44	0.33	0.09	.21	118.82	70.10	.29	52.67	9.63	.40
HFCS	F CON	1.42	0.12		0.27	0.07		147.38	74.92		41.07	5.50	
	F IUGR	1.29	0.09	.42	0.53	0.09	.09	29.44	11.27	.19	46.73	1.27	.37
	M CON	1.28	0.03		0.48	0.07		36.61	15.44		35.00	8.82	
	M IUGR	1.37	0.09	.40	0.31	0.11	.23	157.50	104.55	.32	35.63	6.10	.96
Diff	F CON	0.23	0.08		0.08	0.08		−46.85	93.80		3.90	9.40	
	F IUGR	0.41	0.03	**.082**	0.23	0.20	.509	−147.43	137.84	.58	13.13	2.58	.40
	M CON	0.35	0.04		0.00	0.11		3.55	22.85		−8.03	6.58	
	M IUGR	0.29	0.12	.66	−0.02	0.17	.92	38.68	151.16	.83	−17.03	4.22	.31

(Table 1). The 7-week average for urine volume, urine creatinine, and urine sodium was greater, while urine potassium was marginally less in IUGR versus CON females (Table 2). Serum measures of creatinine, aldosterone, and cortisol were similar in IUGR and CON females (Table 3). On average for the HFCS challenge, urine potassium excretion was lower in IUGR than CON females (Table 2).

In IUGR versus CON males, food and fructose drink consumption were similar during the HFCS challenge. IUGR males' weight and BMI after the challenge were similar to CON males. The change in BMI from after challenge to baseline showed an increase in IUGR and decrease in CON males (Table 1). The 7-week average for urine volume, urine creatinine, urine potassium, urine sodium, serum creatinine, aldosterone, and cortisol were similar between IUGR and CON (Tables 2 and 3), and showed a similar response to HFCS for systolic, diastolic, and mean arterial blood pressure, and heart rate (Table 4).

3.4.2 | Renal transcriptome

CON females HFCS vs chow
Three-hundred-forty-nine genes were differentially expressed in CON females fed HFCS versus chow: 133 were down and 216 were up (Table S6). Two pathways passed end-of-pathway criteria with one up and one down (Table S2). Nine networks were inhibited and 8 activated (Figure 5, Table S3). Genes in all 17 networks overlap with genes in the 3 canonical pathways. Genes in the networks have roles in multiple canonical pathways including prothrombin activation, fatty acid biosynthesis, Wnt/β-catenin signaling, cyclins, and cell cycle regulation (Table S3).

IUGR females HFCS vs chow
Seven-hundred-ninety-three genes were differentially expressed in IUGR females fed HFCS versus chow: 447 were down and 346 were up (Table S6). Seven pathways passed end-of-pathway criteria—all down, including mTOR, which activates autophagy (Figure 6), eIF4 & p70S6K, and PI3K/AKT signaling. One network with regulator SMARCA4 was activated (Figure 7); genes in this network are included in canonical pathways glucocorticoid receptor, eNOS, oxidative stress response, calcium, and integrin signaling (Table S3).
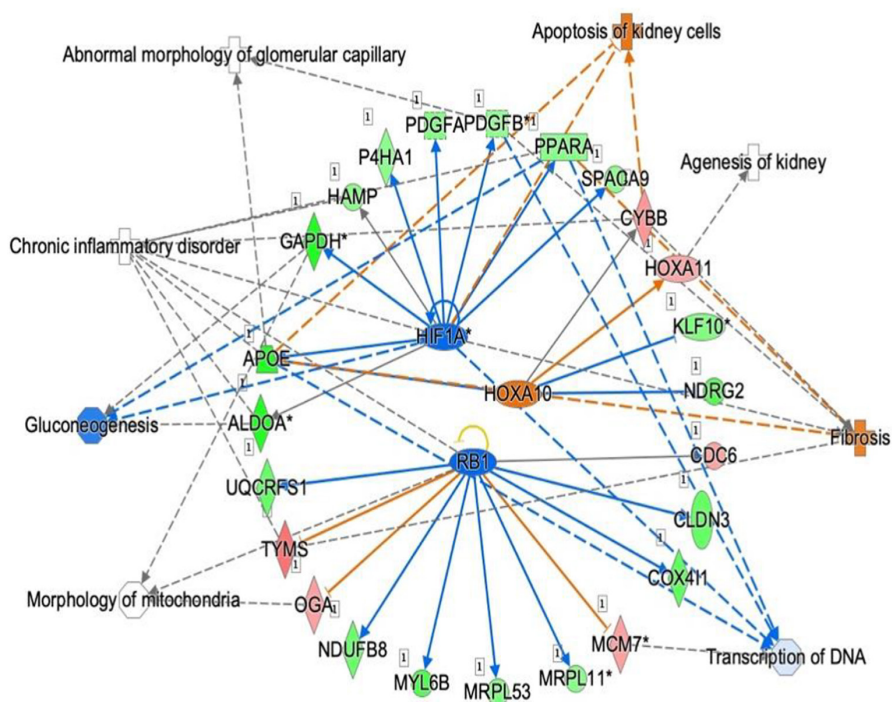
CON males HFCS vs chow
Nine-hundred-fifty-nine genes were differentially expressed in CON males fed HFCS compared with chow: 354 were down and 605 were up (Table S6). Eight pathways passed end-of-pathway criteria—all were up, including cholesterol biosynthesis, and integrin and ILK signaling (Table S2). Of the 5 regulatory networks, 3 were activated by CREB1, AR, and SRF (Figure 7). Genes in each network overlapped with genes in 6 pathways. Genes in these networks have roles in corticotropin-releasing hormone, cholesterol biosynthesis, glucocorticoid receptor, and integrin signaling (Table S3).

TABLE 4 Heart rate and blood pressure

		Heart rate (BPM)			Mean blood pressure (mg/Hg)			Systolic blood pressure (mg/Hg)			Diastolic blood pressure (mg/Hg)		
		Mean	SEM	*p*-Value	Mean	SEM	*p*-Value	Mean	SEM	*p*-Value	Mean	SEM	*p*-Value
M CON	Chow	114.48	6.89		96.89	6.32		115.92	8.28		83.17	4.38	
M IUGR		111.31	1.39	.79	90.26	6.22	.36	107.21	0.67	.37	78.55	0.47	.37
M CON	HFCS	105.34	7.43		88.41	5.60		113.75	3.37		70.89	5.96	
M IUGR		108.47	2.05	.79	81.26	7.67	.27	102.99	0.60	.11	66.87	0.47	.56
M CON	Diff	−9.14	1.72		−8.49	4.91		−2.17	6.27		−12.28	5.90	
M IUGR		−2.84	3.19	.21	−9.00	1.87	.92	−4.22	0.75	.80	−11.68	0.15	.93

FIGURE 3 Renal transcriptome comparison of IUGR vs CON females maintained on chow diet. Merged HIF1A, HOXA10, and RB1 inhibitory regulatory networks in IUGR F vs CON F fed the chow diet. Red fill denotes up-regulated genes, green down-regulated, blue predicted down-regulated, orange predicted up-regulated, gray were not different, and white fill were not detected. Lines with arrows denote activation; lines ending in perpendicular line denote inhibition

IUGR males HFCS vs chow

Twelve-hundred-nine genes were differentially expressed in IUGR males fed HFCS versus chow: 503 were down and 706 were up (Table S6). Two pathways passed end-of-pathway criteria—mitochondrial function was up and assembly of RNA polymerase complex was down (Table S2). Two networks with regulators PARP1 and POU4F1 were inhibited (Figure 8). Genes in these networks have roles in thrombin and glucocorticoid receptor signaling.

3.4.3 | Urine metabolome in IUGR vs CON females and males on HFCS

Thirty-eight metabolites were detected above background in urine from males and females on HFCS (Supplemental S5). Of these, seven metabolites were differentially abundant between females and males with 6 being less abundant in females (Table 8). PCA of these metabolites, revealed group clustering by sex (Figure 2B). Seven of the metabolites detected after the challenge were specific to HFCS (Table 9).

CON females fed HFCS versus chow showed 2 decreased metabolites—hemimellitene and azelaic acid (Table 10). Comparison of IUGR females fed HFCS versus chow revealed 6 marginally different metabolites. Stearic acid showed lower abundance, and all others higher abundance in HFCS versus chow (Table 11). PCA of metabolites present in both IUGR chow and HFCS female urine samples revealed increased separation of clusters versus CON females (Figure S1).

IUGR and CON male urine metabolite abundance was similar on chow. Following HFCS challenge, 4 metabolites were different in IUGR versus CON: N-mehtyl-N-octyl-1-octanamine and N,N-dimethyloctlamine decreased, and hippuric acid and lauric acid increased (Table 12).

4 | DISCUSSION

A poor fetal nutritional environment, due not only to food availability but also poor placental function, followed by a postnatal calorie-rich
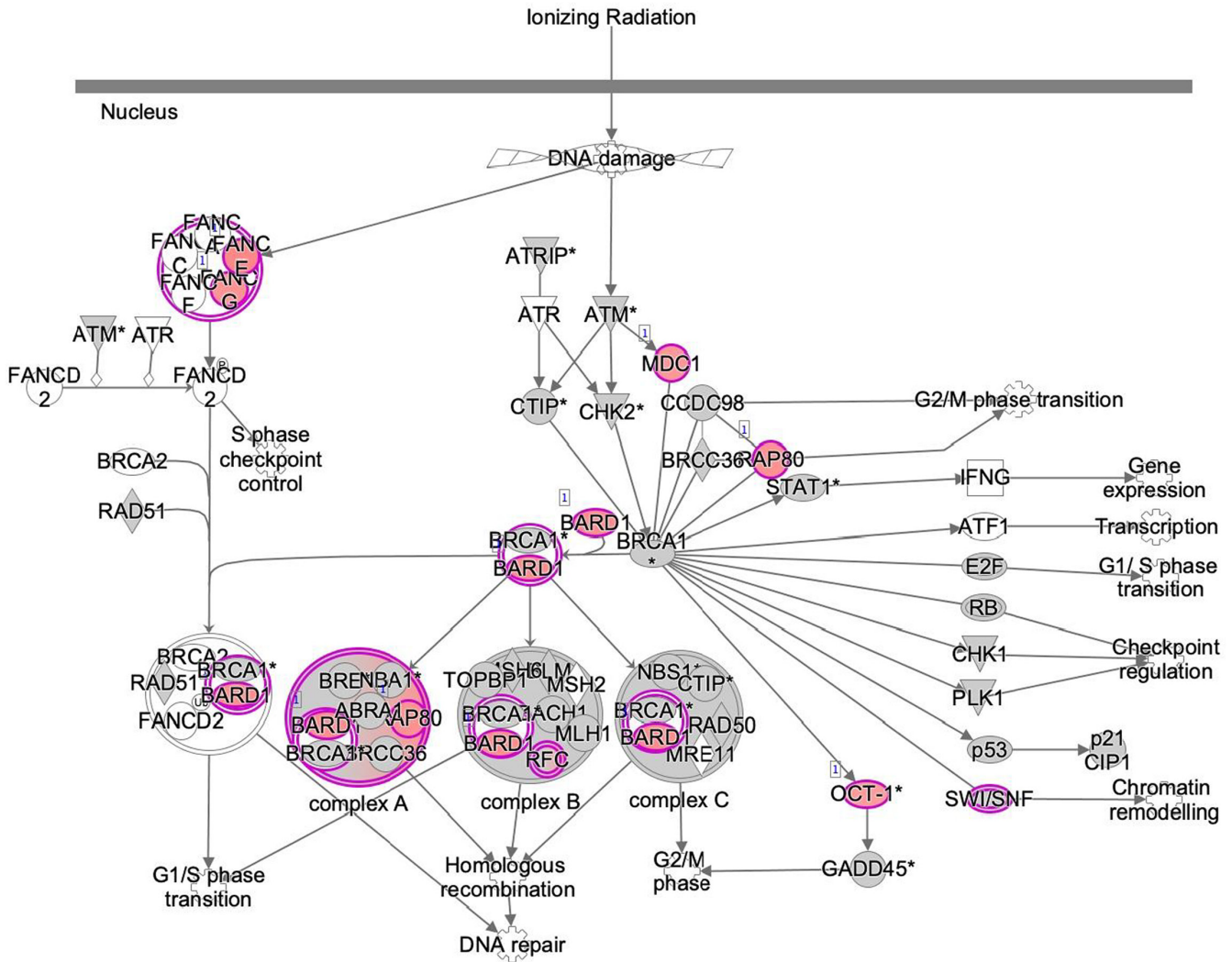
FIGURE 4 Renal transcriptome comparison of IUGR vs CON males maintained on chow diet. Role of BRCA1 in the DNA damage response signaling pathway in IUGR males compared with CON males fed the chow diet. Red fill denotes up-regulated genes in IUGR males compared with CON males, gray fill indicates genes that were not different, and white fill was not detected. Lines with arrows denote activation

TABLE 5 Females vs males chow diet

Metabolite	Fold change	p-Value
Indole-acetic acid	−2.2	6.27E-04
Dihydroferulic acid	−2.9	1.82E-02
Indane	−2.5	1.88E-02
Hemimellitene	−2.7	1.91E-02
Tridecane	−2.6	4.93E-02
Decane	−2.8	4.99E-02
2,4-dichlorobenzoate	−2.6	6.55E-02
Phenyllactic acid	−3.5	9.33E-02

environment is common in developed countries. This prenatal/postnatal caloric mismatch predisposes IUGR offspring to early-onset metabolic dysregulation leading to dyslipidemia and hypertension[44] in juveniles[21,45] and cardiac dysfunction in young adults.[19] Here, we follow-up two questions from our fetal kidney studies: (1) Do fetal MNR effects on kidney growth and function persist postnatally in IUGR offspring; (2) Does a second-hit of caloric mismatch between fetal and postnatal life reveal renal vulnerabilities undetected without the second-hit.

4.1 | Comparison of CON and IUGR prior to the HFCS challenge

Sex differences in transcriptomics analysis of kidney have previously been reported in rodent and human studies.[32,46] Our study in baboons corroborates these reports and therefore males and females we analyzed separately. In postnatal IUGR females, measures of kidney function, gene expression, and metabolite abundance differed from CON females. Signs of renal dysfunction in IUGR females included decreased urine potassium and serum creatinine, and increased urine creatinine.

TABLE 6 Urine metabolites in chow diet only

Common name	HMDB	KEGG	PubChem
Delta Hexalactone	HMDB0000453	NA	13 204
Dihydroferulic acid	HMDB0062121	NA	14 340
Indole-3-propionic acid	HMDB0002302	NA	3744
Tridecane	HMDB0034284	C13834	12 388
3-hydroxy-3-phenylpropanoic acid	HMDB0124925 (predicted)	NA	92 959
Urea	HMDB00294	C00086	1176
3-hydroxy-3-phenylbutan-2-one	NA	NA	233 220
L-Tryptophan	HMDB00929	C00078	6305
Undecanedioic acid	HMDB00888	NA	15 816
Dodecanedioic acid	HMDB0000623	C02678	12 736
Pentadecanoic acid	HMDB0000826	C16537	13 849
Caproic acid	HMDB0000535	C01585	8892
2,4,6,8-Tetramethyl-1-undecene	NA	NA	536 235
Tridecanoic acid	HMDB00910	C17076	12 530
Arachidonic acid	HMDB01043	C00219	444 899
Lignoceric acid	HMDB0002003	C08320	11 197

TABLE 7 IUGR vs CON females on chow

Metabolite	Fold change	p-Value
2-ethyl-p-xylene	1.7	3.89E-02
Decane	1.6	4.44E-02
Hemimellitene	1.6	7.31E-02
Tridecane	2.3	7.66E-02
Indane	1.6	7.68E-02

Our transcriptome analysis of kidney biopsies overlapped with 71.4% of previously reported nephron-specific genes in rodents.[33] supporting the specificity of biopsy procedures. Transcriptomics revealed down-regulation of oxidative phosphorylation and mitochondrial function and inhibition of causal networks regulated by RB1 and HOXA10 in IUGR versus CON. Results indicate that juvenile IUGR female kidneys differ from CON at cellular and molecular levels. Decreased human urinary potassium excretion correlates with reduced renal proximal tubule function.[47,48] Urine metabolomics revealed elevated aromatic hydrocarbons indicating changes in metabolic end-products associated with mitochondrial dysfunction in IUGR females, which is associated with mitochondrial dysfunction in human chronic kidney disease.[49] HIF1A expression, which is down-regulated in IUGR females, is specific to proximal tubule function.[50] In addition, regulators RB1 and HOXA10 are predicted to inhibit mitochondrial function. Together, these suggest that shorter proximal tubules[15] in IUGR females persist postnatally and predisposes to reduced renal function via reduced mitochondrial function.

In males on chow diet, transcriptional pathways related to cell stress and DNA damage were up-regulated in IUGR versus CON. In addition, more than 1600 genes were differentially expressed in IUGR versus CON males (~2.5× more than IUGR versus CON females); however, only 5 pathways passed end-of-pathway criteria, with 3 related to DNA damage. No regulatory networks showed coordinated outcomes. The large number of differentially expressed genes with lack of enrichment in coordinated pathways in IUGR males indicates significant renal molecular dysregulation.

4.2 | Comparison of CON and IUGR response to HFCS

To address the question whether the second-hit by nutritional mismatch between fetal and postnatal life reveals renal vulnerabilities in juvenile primates, we compared IUGR and CON before and after the HFCS diet.

IUGR females had lower weights and BMIs than CON after the 7-week challenge. The 7-week average increases in urine creatinine and sodium in IUGR females suggest early preclinical kidney dysfunction. CON females' transcriptome response to the HFCS challenge revealed coordinated expression including activation of SREBF1 and SREBF2 networks, and Wnt/β-catenin signaling which are responsive to ER stress,[51] renal cholesterol synthesis,[52] and fatty acid biosynthesis, respectively. IUGR females' transcriptome response included down-regulation of nutrient-sensing pathway mTOR, indicating persistence of fetal kidney decreased mTOR signaling.[15,16] In addition, inhibition of mTOR signaling causes activation of autophagy. Autophagy activation is critical for podocyte function and health, and is an indicator of podocyte injury common to multiple kidney diseases.[53] Our finding that mTOR signaling is inhibited with activation of autophagy in IUGR female response to the HFHS diet, is consistent with response to kidney injury. This response is not observed in CON females or in either group of males. We also found up-regulation of the SMARCA4 network, central to
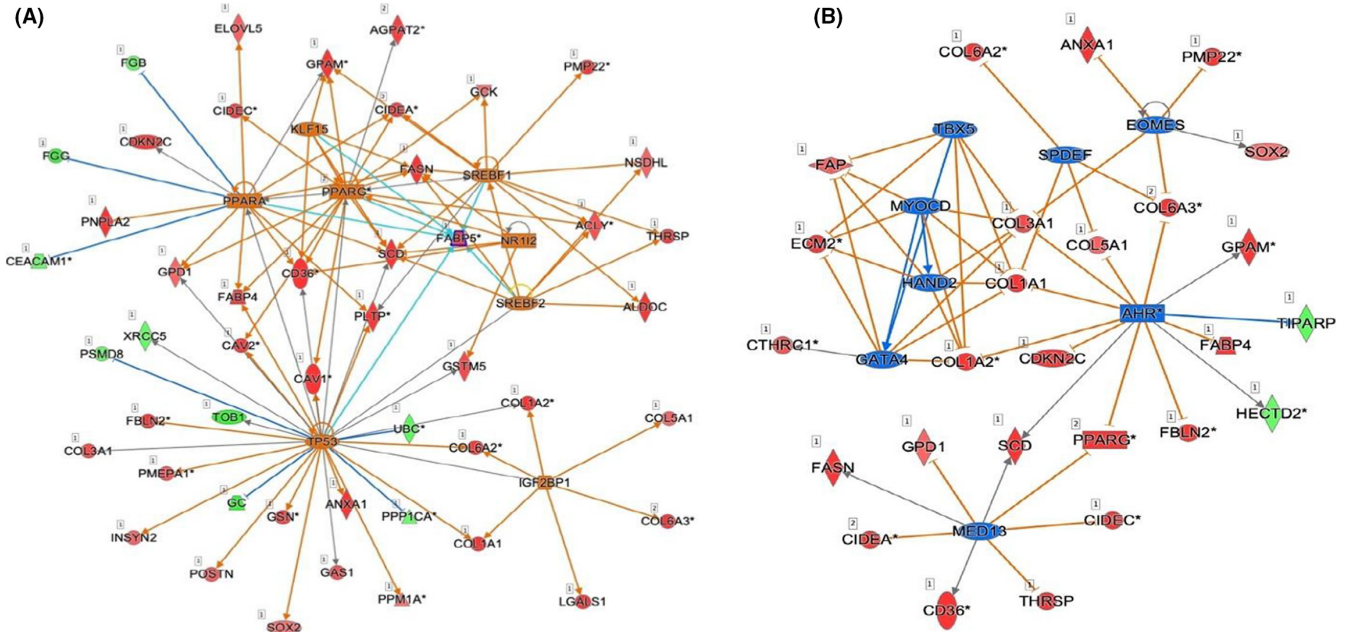
(A)

(B)

FIGURE 5 Renal transcriptome comparison of CON females fed the HFCS diet compared with chow diet. Activated (A) and inhibited (B) regulatory networks in CON females fed the HFCS diet versus chow diet. Red fill denotes up-regulated genes, green down-regulated, blue predicted down-regulated, orange predicted up-regulated, gray were not different, and white fill were not detected. Lines with arrows denote activation; lines ending in perpendicular line denote inhibition
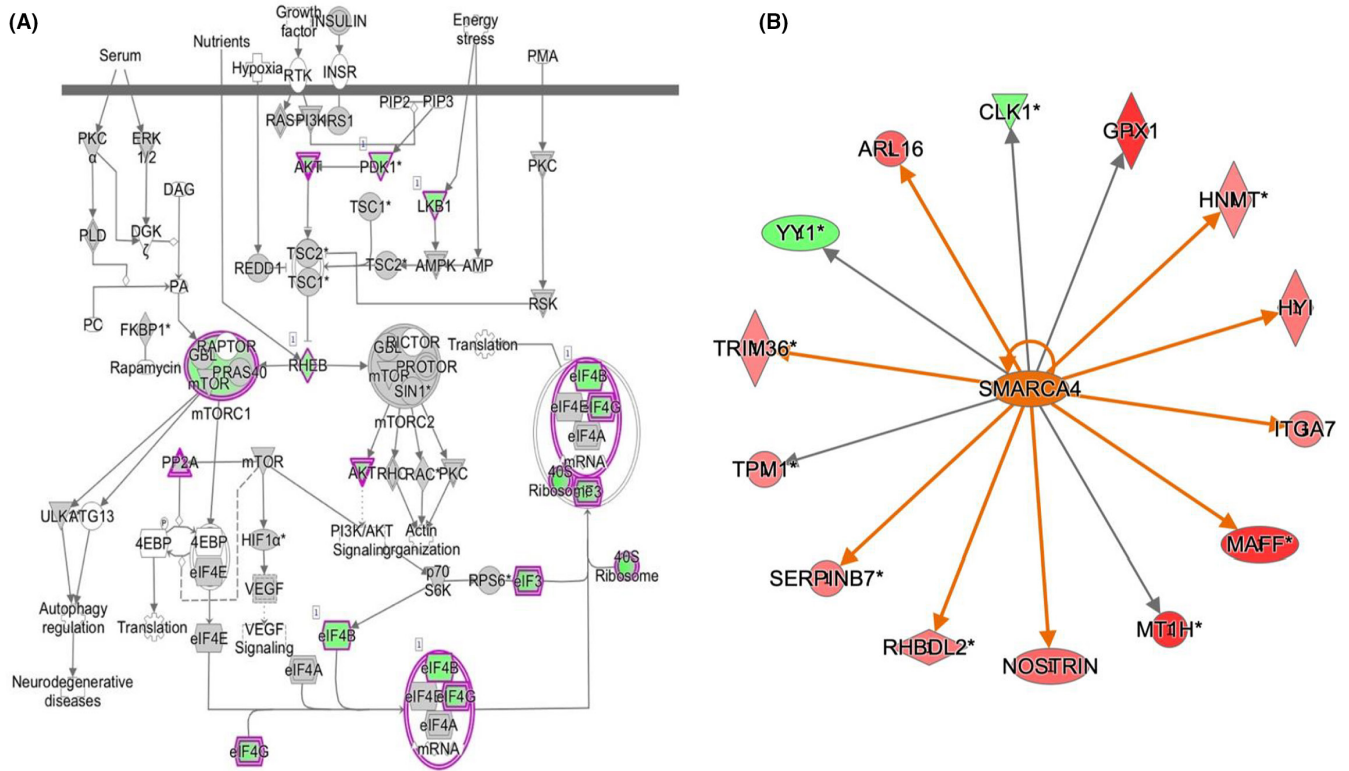
(A)

(B)

FIGURE 6 Renal transcriptome comparison of IUGR females fed the HFCS diet compared with chow diet. (A) Down regulation of mTOR signaling in renal transcriptome of IUGR females fed the HFCS diet compared with chow diet. Green fill denotes down-regulated genes in IUGR females compared with CON females, gray fill indicates genes that were not different, and white fill were not detected. Lines with arrows denote activation; lines ending in perpendicular line denote inhibition. (B) Activation of SMARCA4 regulatory network in renal transcriptome of IUGR females fed the HFCS diet compared with chow diet. Red fill denotes up-regulated genes, green down-regulated, and orange predicted up-regulated

FIGURE 7 Renal transcriptome comparison of CON males fed the HFCS diet compared with chow diet. Merged CREB1, AR, and SRF activated regulatory networks in CON males fed the HFCS diet versus chow diet. Red fill denotes up-regulated genes, green down-regulated, and orange predicted up-regulated. Lines with arrows denote activation; lines ending in perpendicular line denote inhibition
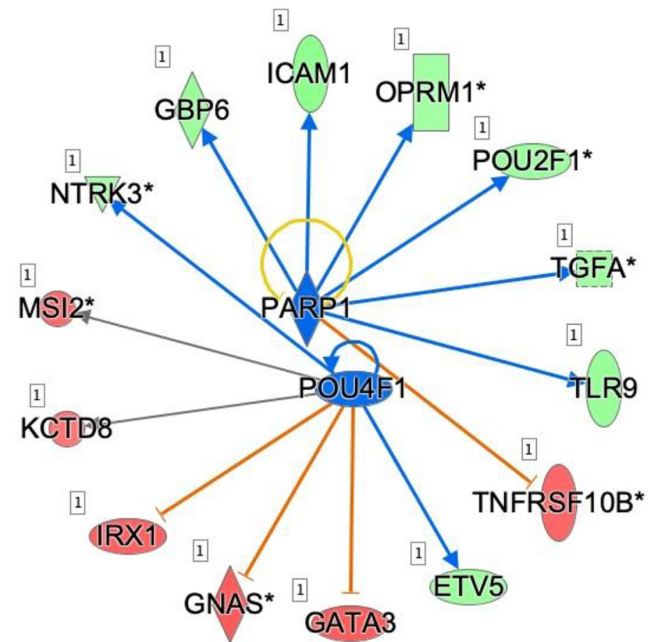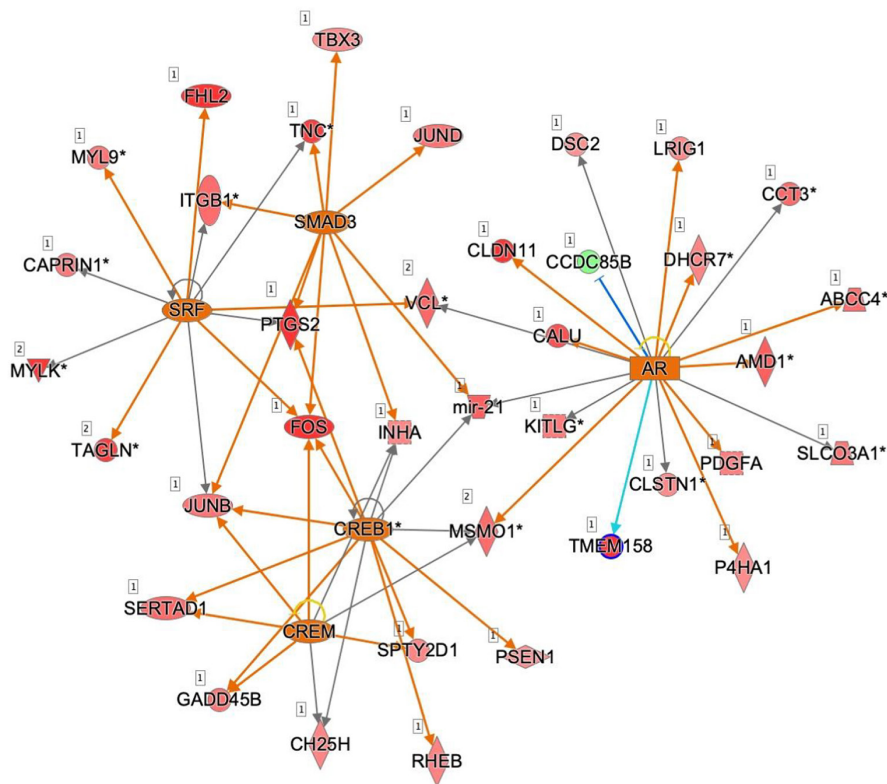

FIGURE 8 Renal transcriptome comparison of IUGR males fed the HFCS diet compared with chow diet. Merged PARP1 and POU4F1 inhibited regulatory networks in IUGR males fed the HFCS diet versus chow diet. Red fill denotes up-regulated genes, green down-regulated, and blue predicted down-regulated. Lines with arrows denote activation; lines ending in perpendicular line denote inhibition

TABLE 8 Females vs males on HFCS diet

Metabolite	Fold change	p-Value
Indole-acetic acid	−4.365	4.00E-03
Azelaic acid	−3.036	8.07E-03
Hippuric acid	−5.323	1.27E-02
Prehnitene	−1.639	1.42E-02
Hemimellitene	−1.550	2.82E-02
Indane	−1.734	3.03E-02
N,N-dimethyl-1-Pentadecanamine	1.906	4.84E-02

TABLE 9 Diet-specific metabolites - urine metabolites in HFCS diet only

Common name	HMDB ID	KEGG ID	PubChem ID
(S)3-hydroxyisobutyric acid (3-HIBA)	HMDB0000023	C06001	440873
Prehnitene	HMDB0059823	NA	10236
4-Hydroxyphenylpyruvic acid (4-HPPA)	HMDB0000707	C01179	979
3-t-Pentylcyclopentanone	NA	NA	551379
6-methyl-2-Hepten-4-one	NA	NA	12502788
4-methylcatechol	HMDB0000873	C06730	9958
Mercaptoacetic acid	NA	C02086	1133

DNA damage response,[54] oxidative damage,[55] and tissue remodeling,[56] suggests renal fibrosis in IUGR females.

In response to the HFCS, CON males' transcriptome showed up-regulation of cholesterol synthesis and activation of a CREB1

network; CREB1 activates proximal tubule sodium and fluid transport.[57] The androgen receptor (AR) network was also activated; androgens in blood and intrarenal synthesis[58] can bind to distal tubular AR cells, increasing epithelial sodium transport.[59] SRF, one regulator

TABLE 10 CON females on HFCS vs chow diet

Metabolite	Fold change	p-Value
Hemimellitene	1.8	2.12E-02
Azelaic acid	−1.5	3.04E-02
Decane	2.0	5.61E-02
Pyrocatechol	2.7	6.22E-02

TABLE 11 IUGR females on HFCS vs chow diet

Metabolite	Fold change	p-Value
Hemimellitene	1.4	5.83E-02
Stearic acid	−7.3	5.12E-02
N,N-dimethyloctylamine	5.1	5.72E-02
Lauric acid	2.7	6.23E-02
Indane	1.4	5.86E-02
Hydrocinnamic acid	1.6	8.64E-02

TABLE 12 IUGR vs CON males on HFCS diet

Metabolite	Fold change	p-Value
N-methyl-N-octyl-1-Octanamine	1.01	4.22E-03
N,N-Dimethyloctylamine	1.01	3.16E-02
Hippuric acid	−1.03	3.26E-02
Lauric acid	−1.00	4.90E-02

in this network, is involved in maintenance of podocyte structure and function.[60] These results indicate CON male kidneys respond to the HFCS diet. Unlike CON males, IUGR males showed no coordinated renal molecular response to HFCS. IUGR males diet response revealed 1209 differentially expressed genes, ~25% more than CON males' response and ~50% more than IUGR females. In spite of the larger number of differentially expressed genes in IUGR males compared with all other groups, only 2 pathways passed end-of-pathway criteria—mitochondrial function and assembly of RNA polymerase complex, and only one network—PARP1, was identified. PARP inhibition is vasoprotective in models of renal failure.[61]

We identified diet-specific urine metabolites. Metabolites 3-hydroxyisobutyric acid (3-HIBA) and 4-hydroxyphenylpyruvic acid (4-HPPA) were observed in HFCS samples and may have inhibitory effects on mitochondrial creatine kinase activity[62] and homeostasis,[63] and the former is associated with diabetic kidney disease.[49] Urine metabolomic analysis showed increased presence of methylated metabolites for the HFCS versus chow for both IUGR and CON, suggesting HFCS diet alters overall methylation status of metabolites and DNA.[64] Take together, these findings indicate the need to evaluate the IUGR and CON epigenome before and after HFSC challenge as a potential mechanism regulating transcriptional response to HFCS.

Although we saw differences between IUGR and CON male response to HFCS at the molecular level, both gene expression and metabolite abundance, we did not find differences in measures of renal function, blood pressure, or heart rate. Few of the studies that have evaluated renal function in mammalian IUGR juvenile offspring demonstrated catch-up growth. Study of IUGR juvenile sheep found catch-up growth in response to an energy-dense diet and decreased nephron numbers.[65] Importantly, in agreement with our blood pressure data from males, they found no evidence of hypertension. It is possible that clinical effects of IUGR on kidney function do not manifest during the juvenile period due to large metabolic demands of rapid growth. It is also possible that a 7-week challenge is too short to impact blood pressure or at this young age NHP kidneys are able to compensate.

In conclusion, this study showed that in utero renal effects of MNR persist in postnatal IUGR juvenile primates. Additionally, a second metabolic hit revealed sex-specific renal vulnerabilities beyond those programmed by IUGR alone and indicated reduced kidney function, altered urine metabolome and renal transcriptome activity, consistent with impaired nutrient sensing and findings of MNR effects on fetal primate kidneys. Exposure to the HFCS challenge resulted in renal transcriptome changes, suggesting a lack of coordinated molecular response with IUGR. Longer term study as animals age is required to determine whether molecular changes observed in this study manifest as impairment of kidney function in IUGR offspring as adults.

CONFLICT OF INTEREST
The authors have no potential financial conflicts of interest.

DATA AVAILABILITY STATEMENT
The data that support the findings of this study are openly available in NCBI Gene Expression Omnibus database at http://www.ncbi.nlm.nih.gov/geo/, reference number GSE149895.

ORCID
Andrew C. Bishop https://orcid.org/0000-0003-0534-0859
Edward J. Dick Jr https://orcid.org/0000-0003-2373-7921
Laura A. Cox https://orcid.org/0000-0002-8836-3783

REFERENCES
1. Gurusinghe S, Tambay A, Sethna CB. Developmental origins and nephron endowment in hypertension. *Front Pediatr.* 2017;5:151.
2. Luyckx VA, Brenner BM. Birth weight, malnutrition and kidney-associated outcomes—a global concern. *Nat Rev Nephrol.* 2015;11(3):135-149.
3. Luyckx VA, Brenner BM. Clinical consequences of developmental programming of low nephron number. *Anat Rec (Hoboken).* 2020;303:2613-2631.
4. O'Dowd R, Kent JC, Moseley JM, Wlodek ME. Effects of uteroplacental insufficiency and reducing litter size on maternal mammary function and postnatal offspring growth. *Am J Physiol Regul Integr Comp Physiol.* 2008;294(2):R539-R548.

5. Breuss JM, Gallo J, DeLisser HM, et al. Expression of the beta 6 integrin subunit in development, neoplasia and tissue repair suggests a role in epithelial remodeling. *J Cell Sci*. 1995;108(Pt 6):2241-2251.

6. Armitage JA, Khan IY, Taylor PD, Nathanielsz PW, Poston L. Developmental programming of the metabolic syndrome by maternal nutritional imbalance: how strong is the evidence from experimental models in mammals? *J Physiol*. 2004;561(Pt 2):355-377.

7. Langley-Evans SC. Fetal programming of cardiovascular function through exposure to maternal undernutrition. *Proc Nutr Soc*. 2001;60(4):505-513.

8. Stocker CJ, Arch JR, Cawthorne MA. Fetal origins of insulin resistance and obesity. *Proc Nutr Soc*. 2005;64(2):143-151.

9. Luyckx VA, Bertram JF, Brenner BM, et al. Effect of fetal and child health on kidney development and long-term risk of hypertension and kidney disease. *Lancet*. 2013;382(9888):273-283.

10. Andersen MC, Engström PG, Lithwick S, et al. In silico detection of sequence variations modifying transcriptional regulation. *PLoS Comput Biol*. 2008;4(1):e5.

11. Coleman-Jensen A, Gregory C, Singh A. Household food security in the United States in 2013. USDA-ERS Economic Research. *Report*. 2014;173:1-41.

12. Godfrey KM, Lillycrop KA, Burdge GC, Gluckman PD, Hanson MA. Epigenetic mechanisms and the mismatch concept of the developmental origins of health and disease. *Pediatr Res*. 2007;61(5 Pt 2):5R-10R.

13. Gallo LA, Tran M, Moritz KM, Wlodek ME. Developmental programming: variations in early growth and adult disease. *Clin Exp Pharmacol Physiol*. 2013;40(11):795-802.

14. Rabadan-Diehl C, Nathanielsz P. From Mice to Men: research models of developmental programming. *J Dev Orig Health Dis*. 2013;4(1):3-9.

15. Cox LA, Nijland MJ, Gilbert JS, et al. Effect of 30 per cent maternal nutrient restriction from 0.16 to 0.5 gestation on fetal baboon kidney gene expression. *J Physiol*. 2006;572(Pt 1):67-85.

16. Nijland MJ, Schlabritz-Loutsevitch NE, Hubbard GB, Nathanielsz PW, Cox LA. Non-human primate fetal kidney transcriptome analysis indicates mammalian target of rapamycin (mTOR) is a central nutrient-responsive pathway. *J Physiol*. 2007;579(Pt 3):643-656.

17. Pereira SP, Oliveira PJ, Tavares LC, et al. Effects of moderate global maternal nutrient reduction on fetal baboon renal mitochondrial gene expression at 0.9 gestation. *Am J Physiol Renal Physiol*. 2015;308(11):F1217-F1228.

18. Unterberger A, Szyf M, Nathanielsz PW, Cox LA. Organ and gestational age effects of maternal nutrient restriction on global methylation in fetal baboons. *J Med Primatol*. 2009;38(4):219-227.

19. Kuo AH, Li C, Li J, Huber HF, Nathanielsz PW, Clarke GD. Cardiac remodelling in a baboon model of intrauterine growth restriction mimics accelerated ageing. *J Physiol*. 2017;595(4):1093-1110.

20. Hellmuth C, Uhl O, Kirchberg FF, et al. Influence of moderate maternal nutrition restriction on the fetal baboon metabolome at 0.5 and 0.9 gestation. *Nutr Metab Cardiovasc Dis*. 2016;26(9):786-796.

21. Choi J, Li C, McDonald TJ, et al. Emergence of insulin resistance in juvenile baboon offspring of mothers exposed to moderate maternal nutrient reduction. *Am J Physiol Regul Integr Comp Physiol*. 2011;301(3):R757-R762.

22. Guo C, Li C, Myatt L, Nathanielsz PW, Sun K. Sexually dimorphic effects of maternal nutrient reduction on expression of genes regulating cortisol metabolism in fetal baboon adipose and liver tissues. *Diabetes*. 2013;62(4):1175-1185.

23. Nijland MJ, Mitsuya K, Li C, et al. Epigenetic modification of fetal baboon hepatic phosphoenolpyruvate carboxykinase following exposure to moderately reduced nutrient availability. *J Physiol*. 2010;588(Pt 8):1349-1359.

24. Kamat A, Nijland MJ, McDonald TJ, et al. Moderate global reduction in maternal nutrition has differential stage of gestation specific

effects on {beta}1- and {beta}2-adrenergic receptors in the fetal baboon liver. *Reprod Sci*. 2011;18(4):398-405.

25. Li C, Ramahi E, Nijland MJ, et al. Up-regulation of the fetal baboon hypothalamo-pituitary-adrenal axis in intrauterine growth restriction: coincidence with hypothalamic glucocorticoid receptor insensitivity and leptin receptor down-regulation. *Endocrinology*. 2013;154(7):2365-2373.

26. Li C, Schlabritz-Loutsevitch NE, Hubbard GB, et al. Effects of maternal global nutrient restriction on fetal baboon hepatic insulin-like growth factor system genes and gene products. *Endocrinology*. 2009;150(10):4634-4642.

27. Nijland M, Schalbritz-Loutsevitch N, Hubbard G, et al. Nonhuman Primate Fetal Kidney Transcriptome Analysis Indicates mTOR is a Central Nutrient Responsive Pathway. *J Phys*. 2007;579:643-656.

28. Schlabritz-Loutsevitch NE, Howell K, Rice K, et al. Development of a system for individual feeding of baboons maintained in an outdoor group social environment. *J Med Primatol*. 2004;33(3):117-126.

29. Higgins PB, Bastarrachea RA, Lopez-Alvarenga JC, et al. Eight week exposure to a high sugar high fat diet results in adiposity gain and alterations in metabolic biomarkers in baboons (Papio hamadryas sp.). *Cardiovasc Diabetol*. 2010;9:71.

30. Gallo LA, Tran M, Cullen-McEwen LA, et al. Transgenerational programming of fetal nephron deficits and sex-specific adult hypertension in rats. *Reprod Fertil Dev*. 2014;26(7):1032-1043.

31. Eriksson JG, Salonen MK, Kajantie E, Osmond C. Prenatal Growth and CKD in Older Adults: Longitudinal Findings From the Helsinki Birth Cohort Study, 1924-1944. *Am J Kidney Dis*. 2018;71(1):20-26.

32. Cooke CL, Zhao L, Gysler S, Arany E, Regnault TRH. Sex-specific effects of low protein diet on in utero programming of renal G-protein coupled receptors. *J Dev Orig Health Dis*. 2014;5(1):36-44.

33. Clark JZ, Chen L, Chou CL, Jung HJ, Lee JW, Knepper MA. Representation and relative abundance of cell-type selective markers in whole-kidney RNA-Seq data. *Kidney Int*. 2019;95(4):787-796.

34. Shade RE, Blair-West JR, Carey KD, Madden LJ, Weisinger RS, Denton DA. Synergy between angiotensin and aldosterone in evoking sodium appetite in baboons. *Am J Physiol Regul Integr Comp Physiol*. 2002;283(5):R1070-R1078.

35. Spradling-Reeves KD, Glenn JP, Lange KJ, et al. The non-human primate kidney transcriptome in fetal development. *J Med Primatol*. 2018;47(3):157-171.

36. Spradling KD, Glenn JP, Garcia R, Shade RE, Cox LA. The baboon kidney transcriptome: analysis of transcript sequence, splice variants, and abundance. *PLoS One*. 2013;8(4):e57563.

37. Kramer A, Green J, Pollard J Jr, et al. Causal analysis approaches in Ingenuity Pathway Analysis. *Bioinformatics*. 2014;30(4):523-530.

38. Heim J. *Small Molecule Metabolite Identifications in Diabetic Versus Non-Diabetic Urine Sample Groups Using Comprehensive Two-Dimensional Gas Chromatography Combined with Time-of-Flight Mass Spectrometry (GCxGC-TOFMS)*. LECO Corporation; 2008 Contract No.: 203-821-354.

39. Sumner LW, Amberg A, Barrett D, et al. Proposed minimum reporting standards for chemical analysis Chemical Analysis Working Group (CAWG) Metabolomics Standards Initiative (MSI). *Metabolomics*. 2007;3(3):211-221.

40. Ramaker RC, Gordon ER, Cooper SJ. R2DGC: threshold-free peak alignment and identification for 2D gas chromatography-mass spectrometry in R. *Bioinformatics*. 2018;34(10):1789-1791.

41. Wishart DS, Feunang YD, Marcu A, et al. HMDB 4.0: the human metabolome database for 2018. *Nucleic Acids Res*. 2018;46(D1):D608-D617.

42. Kanehisa M. Enzyme Annotation and Metabolic Reconstruction Using KEGG. *Methods Mol Biol*. 2017;1611:135-145.

43. Chong J, Soufan O, Li C, et al. MetaboAnalyst 4.0: towards more transparent and integrative metabolomics analysis. *Nucleic Acids Res*. 2018;46(W1):W486-W494.

44. Victora CG, Adair L, Fall C, et al. Maternal and child undernutrition: consequences for adult health and human capital. *Lancet*. 2008;371(9609):340-357.

45. Bishop, AC, Libardoni, M, Choudary, A, Misra B, Lange K, Bernal J, Nijland M, Li C, Olivier M, Nathanielsz PW, Cox LA Nonhuman primate breath volatile organic compounds associate with developmental programming and cardio-metabolic status. *J Breath Res* 2018;12(3):036016.

46. Huang L, Liao J, He J, et al. Single-cell profiling reveals sex diversity in human renal proximal tubules. *Gene*. 2020;752:144790.

47. Palmer BF. Regulation of Potassium Homeostasis. *Clin J Am Soc Nephrol*. 2015;10(6):1050-1060.

48. Ueda Y, Ookawara S, Ito K, et al. Changes in urinary potassium excretion in patients with chronic kidney disease. *Kidney Res Clin Pract*. 2016;35(2):78-83.

49. Sharma K, Karl B, Mathew AV, et al. Metabolomics reveals signature of mitochondrial dysfunction in diabetic kidney disease. *J Am Soc Nephrol*. 2013;24(11):1901-1912.

50. Thiagarajan RD, Cloonan N, Gardiner BB, et al. Refining transcriptional programs in kidney development by integration of deep RNA-sequencing and array-based spatial profiling. *BMC Genomics*. 2011;12(1):441.

51. Chiappisi E, Ringseis R, Eder K, Gessner DK. Effect of endoplasmic reticulum stress on metabolic and stress signaling and kidney-specific functions in Madin-Darby bovine kidney cells. *J Dairy Sci*. 2017;100(8):6689-6706.

52. Aboudehen K, Kim MS, Mitsche M, et al. Transcription factor hepatocyte nuclear factor-1beta regulates renal cholesterol metabolism. *J Am Soc Nephrol*. 2016;27(8):2408-2421.

53. Teh YM, Mualif SA, Lim SK. A comprehensive insight into autophagy and its potential signaling pathways as a therapeutic target in podocyte injury. *Int J Biochem Cell Biol*. 2022;143:106153.

54. Rother MB, van Attikum H. DNA repair goes hip-hop: SMARCA and CHD chromatin remodellers join the break dance. *Philos Trans R Soc Lond B Biol Sci*. 2017;372(1731). doi:10.1098/rstb.2016.0285

55. Wu PJ, Chen JB, Lee WC, et al. Oxidative stress and nonalcoholic fatty liver disease in hemodialysis patients. *Biomed Res Int*. 2018;2018:3961748.

56. Savill SA, Leitch HF, Harvey JN, Thomas TH. Functional structure of the promoter regions for the predominant low molecular weight isoforms of tropomyosin in human kidney cells. *J Cell Biochem*. 2012;113(11):3576-3586.

57. Li XC, Zhuo JL. Phosphoproteomic analysis of AT1 receptor-mediated signaling responses in proximal tubules of angiotensin II-induced hypertensive rats. *Kidney Int*. 2011;80(6):620-632.

58. Quinkler M, Bumke-Vogt C, Meyer B, Bähr V, Oelkers W, Diederich S. The human kidney is a progesterone-metabolizing and androgen-producing organ. *J Clin Endocrinol Metab*. 2003;88(6):2803-2809.

59. Quinkler M, Bujalska IJ, Kaur K, et al. Androgen receptor-mediated regulation of the alpha-subunit of the epithelial sodium channel in human kidney. *Hypertension*. 2005;46(4):787-798.

60. Guo B, Lyu Q, Slivano OJ, et al. Serum Response Factor Is Essential for Maintenance of Podocyte Structure and Function. *J Am Soc Nephrol*. 2018;29(2):416-422.

61. Wang C, Xu W, An J, et al. Poly(ADP-ribose) polymerase 1 accelerates vascular calcification by upregulating Runx2. *Nat Commun*. 2019;10(1):1203.

62. Viegas CM, da Costa Ferreira G, Schuck PF, et al. Evidence that 3-hydroxyisobutyric acid inhibits key enzymes of energy metabolism in cerebral cortex of young rats. *Int J Dev Neurosci*. 2008;26(3-4):293-299.

63. Schlattner U, Tokarska-Schlattner M, Wallimann T. Mitochondrial creatine kinase in human health and disease. *Biochim Biophys Acta*. 2006;1762(2):164-180.

64. Showalter MR, Cajka T, Fiehn O. Epimetabolites: discovering metabolism beyond building and burning. *Curr Opin Chem Biol*. 2017;36:70-76.

65. Muhle A, Muhle C, Amann K, et al. No juvenile arterial hypertension in sheep multiples despite reduced nephron numbers. *Pediatr Nephrol*. 2010;25(9):1653-1661.

SUPPORTING INFORMATION

Additional supporting information can be found online in the Supporting Information section at the end of this article.